ORTHOPINAKIOLITE, $Me_{2.95}O_2[BO_3]$†: ITS CRYSTAL STRUCTURE AND RELATIONSHIP TO PINAKIOLITE, $Me_{2.90}O_2[BO_3]$*

YOSHIO TAKÉUCHI, NOBUHIKO HAGA,

Mineralogical Institute, Faculty of Science, University of Tokyo, Hongo, Tokyo 113, Japan

TOSHIO KATO AND YASUNORI MIURA

*Institute of Mineralogical Sciences, Faculty of Literature and Science, Yamaguchi University,
Yoshida, Yamaguchi 753, Japan*

ABSTRACT

The crystal structure of orthopinakiolite, a 18.357(4), b 12.591(2), c 6.068(1) Å, $Pnnm$, has been determined, and yields the cell formula 16 $Me_{3-x}O_2[BO_3]$, where $x = 0.05$, $Me_{3-x} = (Mg_{1.423}Mn^{2+}_{0.432}Fe^{3+}_{0.220}Mn^{3+}_{0.875})_{\Sigma=2.95}$, $Mn^{3+}/Me^{2+} = 0.47$. The mode of cation ordering and the vacancy distribution are primarily explicable from the Jahn-Teller distortion and resulting asymmetric charge distribution about Mn^{3+}. Orthopinakiolite is not a polymorph but an Mn^{3+} (and vacancy)-deficient modification of pinakiolite ($x = 0.1$, $Mn^{3+}/Me^{2+} = 0.56$). The geometrical features of the orthopinakiolite structure can be expressed by Ito cell-twinning of the pinakiolite substructure on the scale of a double Takéuchi cell (a doubled). The polysymmetric synthesis needed to form the Ito "twin" plays a role in reducing the Mn^{3+} (and vacancy) content of the pinakiolite structure. Orthopinakiolite is thus an example of 'tropochemical twinning'.

SOMMAIRE

La structure de l'orthopinakiolite, déterminée pour la maille a 18.357(4), b 12.591(2), c 6.068(1)Å, dans le groupe $Pnnm$, correspond à 16 $Me_{3-x}O_2[BO_3]$ par maille, avec $x = 0.05$, $Me_{3-x} = (Mg_{1.423}Mn^{2+}_{0.432}Fe^{3+}_{0.220}Mn^{3+}_{0.875})_{\Sigma=2.95}$, $Mn^{3+}/Me^{2+} = 0.47$. La mise en ordre des cations et la distribution des lacunes s'expliquent principalement par la distortion Jahn-Teller et la distribution asymétrique des charges correspondante. L'orthopinakiolite est une modification, non pas polymorphique, mais déficiente en Mn^{3+} (et en lacunes), de la pinakiolite ($x = 0.1$, $Mn^{3+}/Me^{2+} = 0.56$). Géometriquement, la structure de l'orthopinakiolite peut s'exprimer par maclage Ito (maclage de mailles) de la sous-structure pinakiolite à l'échelle d'une double maille de Takéuchi (a doublé). La synthèse polysymétrique requise pour former la "macle" d'Ito conduit à une diminution du nombre des ions Mn^{3+} (et des

lacunes) dans la structure de la pinakiolite. L'orthopinakiolite offre donc un exemple de "maclage tropochimique".

(Traduit par la Rédaction)

INTRODUCTION

Ludwigite, pinakiolite, hulsite and orthopinakiolite comprise a family of oxyborates characterized by cations with mixed valence states. Takéuchi *et al.* (1950) determined the essential structural features of warwickite, another oxyborate, ludwigite and pinakiolite, and discussed the common principle governing their morphotropic relations. Series of synthetic borates having these structure types were reported by Bertaut (1950). The crystal structure of vonsenite, a Mg-free ludwigite, confirmed the ludwigite structure, and yielded some additional details of this structure type (Takéuchi 1956, Federico 1957).

Recent structural studies on these minerals and related compounds include those of $FeCoO[BO_3]$, an isotype of warwickite (Venkatakrishnan & Buerger 1972), pinakiolite and warwickite (Moore & Araki 1974), and hulsite (Yamnova *et al.* 1975; Konnert *et al.* 1976). For pinakiolite, Moore & Araki (1974) found a larger cell than that given by Takéuchi *et al.* (1950). The a axis of the new cell corresponds to [101] of the previous cell and is doubled primarily owing to the ordering of certain sets of cations. The new space group, $C2/m$, is different from the previous one, $P2_1/m$, yet both structures share essentially the same geometrical features. This is a consequence of the fact that, if the unit cell in space group $C2/m$ is so folded that its a axis is halved, the resulting symmetry is consistent with $P2_1/m$ but with a halved; the structure given by Takéuchi *et al.* (1950) corresponds to a substructure of the true structure. The relations between the true structure and the substructure were discussed in detail in Moore & Araki (1974).

---

*Dedicated to Professor J. D. H. Donnay on the occasion of his 75th birthday.

†Me: Mg, Mn^{2+}, Mn^{3+}.

Orthopinakiolite has the largest cell (Randmets 1960) among the above mentioned borates, but its structure remained unknown. This mineral is of particular interest because its cell is apparently more closely related to that of ludwigite (*a* and *c* doubled) than to that of pinakiolite (Moore & Araki 1974), even though its structure was first thought to be a derivative of the pinakiolite structure (Randmets 1960). Studies were undertaken to find the structural relationships between these minerals and crystallochemical factors underlying the formation of such a derivative structure. This mineral is also suited to test the partial Patterson method (Takéuchi 1972) as a means of determining the mode of cation ordering in a moderately complex structure.

MATERIAL

Orthopinakiolite crystals from Långban, Sweden, were used for X-ray investigation. In contrast to the platy crystals of pinakiolite, they have a prismatic habit similar to that of ludwigite. Our electron microprobe analyses (Table 1) showed a spatially homogeneous composition and revealed, in addition to Mg and Mn, the presence of Fe and Ca, though the latter was negligible; other elements, *e.g.*, Al and Ti which Irving (in Moore & Araki 1974) detected for pinakiolite, were not found. As will be shown later from the Jahn-Teller distortion of octahedra about Mn^{3+}, it is probable that the unit cell contains at least fourteen Mn^{3+} ions, the number corresponding to 0.875 per five oxygen atoms. On the other hand, Mössbauer spectra of orthopinakiolite (K. Nagashima, priv. comm. 1977) revealed that Fe in this mineral

is mostly in the ferric state; Fe^{2+} is negligible. The Mössbauer evidence then limits approximately the Mn^{3+} content to the above value so as to give a formula in which formal charges are neutralized (Table 1). Orthopinakiolite is thus significantly deficient in Mn^{3+} compared to pinakiolite. This difference is structurally important because the distortions of the octahedra about Mn^{3+} have a significant effect on the neighboring atomic arrangement.

The chemical compositions of these minerals nevertheless share the following features: (1) a general formula, $Me_{3-x}O[BO_3]$, with $x = 0.1$ for pinakiolite, 0.05 for orthopinakiolite, and $Me = Mg$, Mn^{3+}, Mn^{2+}, and (2) compensating for cation deficiencies, excess of cations (other than Mn^{3+}) of higher valencies, like Fe^{3+} or Mn^{4+}, over those reported in the original formula $(Mg_3Mn^{2+})Mn^{3+}{}_2O_4[BO_3]_2$ (Flink 1890, Bäckström 1895).

EXPERIMENTAL

Out of a crystal, a sphere was prepared having a radius of 0.1 mm, and used for X-ray experiments. The cell dimensions obtained from single-crystal diffractometry (graphite-monochromatized Mo $K\alpha$: $\lambda = 0.71069$Å) are: *a* 18.357(4), *b* 12.591(2), *c* 6.068(1)Å, *V* 1402.5Å³. The above-mentioned formula gives a calculated density, $D_x = 4.06$ g·cm⁻³, comparable with the measured value, $D_m = 4.03 \pm 0.05$ (Randmets 1960). The possible space groups are as reported by Randmets (1960): *Pnnm* or *Pnn2*; the former has been confirmed by the structure analysis.

The ω-2θ scan technique was used to measure a total of 3800 independent reflections up to $2\theta = 75°$. Of these, a set of 2309 reflections which had intensities greater than 2σ (I) were used for the structure determination. After due corrections for Lorentz and polarization factors as well as absorption ($\mu = 61.7$ cm⁻¹), the intensities were reduced to structure factors.

STRUCTURE DETERMINATION

As reflections are weak when $l \neq 2n$, the orthopinakiolite structure has a strong pseudo-translation of $c/2$, suggesting a substructure with this half period. This substructure should have a space group *Pbam*, provided it is centrosymmetric. Using a procedure described elsewhere (Takéuchi *et al.* 1950) and a two-dimensional Patterson map, we readily succeeded in deriving the substructure that gave a satisfactory agreement between observed and calculated amplitudes, *F(hk0)*. From the two-dimensional data,

TABLE 1. CHEMICAL COMPOSITIONS OF ORTHOPINAKIOLITE AND PINAKIOLITE

	1	2	3	4
Mg	16.7	16.5	17.4	20.7
Mn	34.4	34.3	39.3	32.0
Fe	5.8	5.9		0.6
Ca	0.0	–		–
Al	–	–		0.7
B		5.17	5.15	5.4
O		38.1	38.15	39.8

1 An average of analyses expressed as element percentages at five sampling points of a crystal from Långban, Sweden, specimen #332376 of the Swedish Museum of Natural History, Stockholm.

2 Theoretical composition: $Mg_{1.423}Mn^{2+}_{0.432}Fe^{3+}_{0.220}Mn^{3+}_{0.875}O_2BO_3$.

3 Composition reported by Bäckström (1895): $(Mg_{1.5}Mn^{2+}_{0.5})Mn^{3+}_{1.00}O_2BO_3$

4 Pinakiolite (Moore & Araki 1974): $Mg_{1.68}Mn^{2+}_{0.09}Fe^{3+}_{0.02}Al^{3+}_{0.05}Mn^{4+}_{0.06}Mn^{3+}_{1.00}O_2BO_3$

TABLE 2. OCCUPANCIES IN THE CATION SITES OF ORTHOPINAKIOLITE

Substructure, *Pbam*				True structure, *Pnmm*						
Site	Number, Wyckoff notation, point symmetry	Occupancy		Site	Number, Wyckoff notation, point symmetry	Occupancy				
		Mg	Mn			Mg	Mn^{2+}	Mn^{3+}	Fe^{3+}	Σ
I	2a, 2/m	--	1.0	M(1)	2a, 2/m	--	--	1.00	--	1.00
				M(2)	2b, 2/m	--	--	1.00	--	1.00
II	2c, 2/m	0.7	0.3	M(3)	2c, 2/m	--	--	1.00	--	1.00
				M(4)	2d, 2/m	0.54(8)	0.05(2)	--	--	1.00+
III	4h, m	0.9	0.1	M(5)	8h, 1	0.918(8)	0.082	--	--	1.00
IV	4g, m	0.25	0.75	M(6)	4g, m	--	--	1.00		1.00
				M(7)	4g, m	--	0.448(7)	--	--	
				M(7*)	4g, m	--	0.26(1)	--	--	1.00
				M(7)	4g, m	--	--	--	0.292(9)	
V	4g, m	0.2	0.8	M(8)	4g, m	--	--	1.00	--	1.00
				M(9)	4g, m	0.57	0.43(1)	--	--	1.00
VI	4h, m	0.7	0.3	M(10)	8h, 1	0.733(8)	0.12**	--	0.147**	1.00
VII	4h, m	0.75	0.25	M(11)	8h, 1	0.775(8)	0.078**	--	0.147**	1.00
				$\sum\limits_{1}^{Z}$ + charge		45.54	13.78	42.00	10.58	111.90
				$\sum\limits_{1}^{Z}$ - charge						112.00

+ Includes 0.41 unoccupied.

** Assumed partition. For calculation, the weighted mean of the Mn^{2+} and Fe^{3+} form factors was used.

and using as cationic form factor, the average of those for Mg and Mn, we refined the structure to $R = 17\%$ to estimate rough contents at the cation sites, on the assumption that there were no vacancies at the cation sites (Table 2).

Note that in the true structure two non-equivalent cations overlap down the *c*-axis projection, at each of the octahedral sites I, II, IV and V (Fig. 1, Table 2). Those which overlap at each of the sites III, VI and VII are equiva-

(a)

(b)
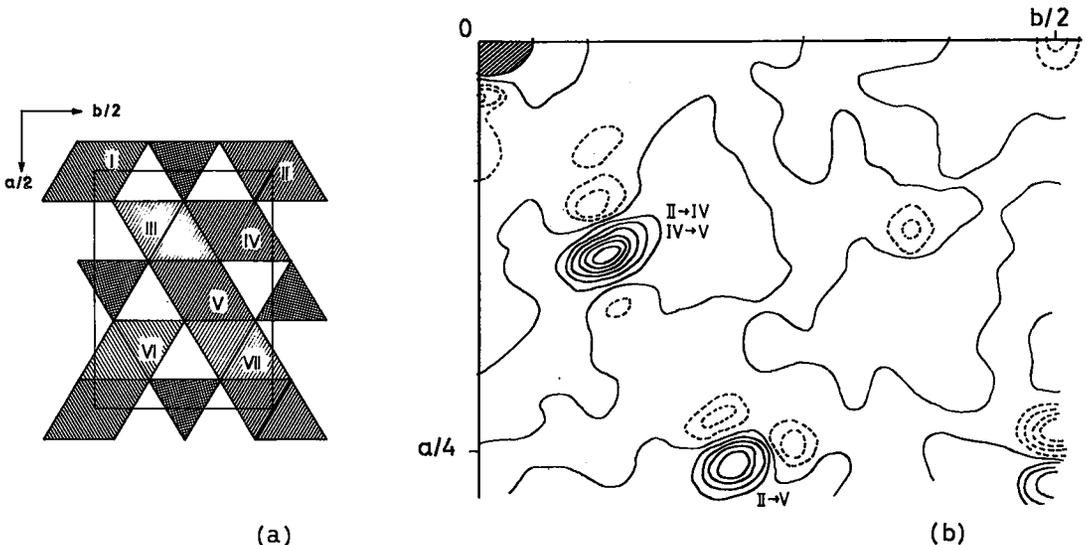
FIG. 1. (a) The *c*-axis projection of the substructure, showing idealized links of regular octahedra (numbers as in Table 2) and BO_3 triangles. The octahedra on the $z = 0$ and $z = 0.5$ levels are ruled, respectively, with heavy and light lines. (b) A portion of the partial Patterson section, $z = 0$, based on the synthesis using only odd terms in l and showing positive peaks due to vectors between octahedral cations II, IV and V.

TABLE 3. POSITIONAL PARAMETERS FOR ORTHOPINAKIOLITE ATOMS

Atom	x	y	z	B(Å²)**
M(1)	0.00000	0.0000	0.0000	0.42
M(2)	.00000	.0000	.5000	.43
M(3)	.00000	.5000	.0000	.48
M(4)	.00000	.5000	.5000	2.4
M(5)	.11890(9)	.1703(1)	.2480(4)	.51
M(6)	.12887(6)	.3935(1)	.0000	.49
M(7)	.1064(2)	.3973(2)	.5000	.98
M(7*)	.144(1)	.3961(8)	.5000	4.8
M(7̄)	.0646(6)	.4043(5)	.5000	3.3
M(8)	.25289(6)	.27535(9)	.0000	.51
M(9)	.2509(1)	.2820(2)	.5000	.79
M(10)	.37222(7)	.1160(1)	.2476(2)	.55
M(11)	.37260(7)	.3948(1)	.2488(3)	.49
B(1)	.9821(4)	.2446(6)	.0000	.40
B(2)	.9816(5)	.2471(7)	.5000	.84
B(3)	.2367(4)	.0318(7)	.0000	.64
B(4)	.2318(4)	.0443(6)	.5000	.59
O(1)	.0662(2)	.0306(3)	.2504(7)	.71
O(2)	.0564(3)	.2416(5)	.0000	.78
O(3)	.0577(3)	.2442(5)	.5000	.75
O(4)	.0731(2)	.4685(3)	.2148(7)	.81
O(5)	.1947(3)	.1234(5)	.0000	.86
O(6)	.1926(3)	.1369(4)	.5000	.73
O(7)	.1802(2)	.3152(3)	.2221(7)	.87
O(8)	.3125(3)	.0407(5)	.0000	.92
O(9)	.3070(3)	.0468(5)	.0000	.77
O(10)	.3189(2)	.2530(3)	.2379(7)	.84
O(11)	.3038(3)	.4466(5)	.0000	.79
O(12)	.2977(3)	.4352(4)	.5000	.72
O(13)	.4463(3)	.1566(5)	.0000	.85
O(14)	.4445(3)	.1595(4)	.5000	.67
O(15)	.4443(3)	.3471(5)	.0000	.74
O(16)	.4423(3)	.3489(4)	.5000	.64

** Calculated from anisotropic thermal parameters.

distortions characteristic of those for Mn^{3+} octahedra and appeared to be fully occupied by that cation. Because of the unexpected result of (ii), a re-examination of cell dimensions was made by taking long-exposure X-ray photographs. However, no extra reflections were observed indicative of a larger cell.

When occupancy parameters at these split positions were introduced in the least-squares calculations, the isotropic refinement converged to $R = 9.0\%$. Subsequent refinement applying anisotropic thermal parameters gave the final value of $R = 4.9\%$ for all reflections. The structure-factor table is available, at a nominal charge, from the Depository of Unpublished Data, CISTI, National Research Council of Canada, Ottawa, Canada, K1A 0S2. The form factors used for Mn^{3+}, Mn^{2+}, Mg^{2+}, B^+ and

TABLE 4. PARAMETERS FOR THE ELLIPSOIDS OF VIBRATION IN ORTHOPINAKIOLITE*

Atom	i	μ_i	θ_{ia}	θ_{ib}	θ_{ic}	Atom	i	μ_i	θ_{ia}	θ_{ib}	θ_{ic}
M(1)	1	0.064	90°	90°	180°	O(3)	1	0.079	174°	84°	90°
	2	0.070	162	72	90		2	0.099	90	90	0
	3	0.082	72	18	90		3	0.112	84	6	90
M(2)	1	0.062	90	90	0	O(4)	1	0.083	39	123	72
	2	0.065	170	80	90		2	0.109	128	139	78
	3	0.090	100	170	90		3	0.109	83	111	158
M(3)	1	0.067	4	94	90	O(5)	1	0.094	161	71	90
	2	0.069	90	90	0		2	0.098	90	90	0
	3	0.096	94	176	90		3	0.119	71	19	90
M(5)	1	0.069	87	82	9	O(6)	1	0.081	90	90	180
	2	0.082	147	122	83		2	0.099	116	26	90
	3	0.090	58	147	84		3	0.107	26	64	90
M(6)	1	0.065	90	90	0	O(7)	1	0.085	159	70	97
	2	0.071	140	50	90		2	0.103	111	158	83
	3	0.097	130	140	90		3	0.123	94	81	10
M(8)	1	0.066	1	91	90	O(8)	1	0.090	167	103	90
	2	0.083	90	90	0		2	0.099	90	90	0
	3	0.090	91	179	90		3	0.131	103	13	90
M(9)	1	0.063	90	90	0	O(9)	1	0.093	163	73	90
	2	0.086	41	49	90		2	0.100	107	163	90
	3	0.137	131	41	90		3	0.104	90	90	0
M(10)	1	0.066	83	104	16	O(10)	1	0.078	39	96	52
	2	0.088	173	90	83		2	0.108	56	110	139
	3	0.093	92	166	104		3	0.119	73	21	102
M(11)	1	0.063	98	84	170	O(11)	1	0.083	57	147	90
	2	0.081	154	116	86		2	0.096	90	90	180
	3	0.090	115	26	81		3	0.117	33	57	90
B(1)	1	0.064	90	90	0	O(12)	1	0.083	40	130	90
	2	0.067	38	52	90		2	0.089	90	90	0
	3	0.082	128	38	90		3	0.113	130	140	90
B(2)	1	0.065	90	90	0	O(13)	1	0.092	133	137	90
	2	0.096	157	67	90		2	0.103	90	90	180
	3	0.136	113	157	90		3	0.115	43	133	90
B(3)	1	0.074	32	58	90	O(14)	1	0.088	91	179	90
	2	0.089	90	90	0		2	0.094	90	90	0
	3	0.103	58	148	90		3	0.094	179	89	90
B(4)	1	0.070	169	79	90	O(15)	1	0.080	90	90	0
	2	0.082	90	90	0		2	0.091	146	56	90
	3	0.103	79	11	90		3	0.115	124	146	90
O(1)	1	0.077	67	78	27	O(16)	1	0.076	90	90	180
	2	0.099	143	113	63		2	0.092	56	34	90
	3	0.106	63	153	89		3	0.100	34	124	90
O(2)	1	0.091	174	84	90						
	2	0.095	90	90	0						
	3	0.111	84	6	90						

* Those for partially occupied sites are not given. $i = \underline{i}$th principal axis; μ_i = rms amplitude (Å); θ_{ia}, θ_{ib}, θ_{ic} = angles between $\underline{i}$th principal axis and the cell axes $\underline{a}$, $\underline{b}$ and $\underline{c}$.

lent by reflection; their contributions to $Fhkl$s having $l = 2n + 1$ would be negligible. As the octahedra that overlap at position I were fully occupied by Mn (Table 2) according to the above preliminary calculations, the next step in determining the structure was to differentiate sets of two cations that overlap respectively at II, IV and V. This was accomplished by the partial Patterson function calculated using only odd-order terms in l.

Among vectors between the sets of cations now considered, those parallel to (001) give positive peaks in the function (Fig. 1), suggesting that all positive-difference electron densities, $\delta(x)$ (Takéuchi 1972) at these positions are in the same level on z, with all negative $\delta(x)$s at the next level. Accordingly, we located Mn at $z = 0$ and Mg at $z = 0.5$ for each of the three sets of positions, thus providing initial phases for $Fhkl$s with $l = 2n + 1$.

Several cycles of isotropic least-squares refinement, utilizing the program LINUS (Coppens & Hamilton 1970), reduced the R value from 35% to 13%. At this stage, we found the following features: (i) the $M(4)$ position was only partly occupied, (ii) the atom at $M(7)$ split to three positions, and (iii) $M(1)$, $M(2)$, $M(3)$, $M(6)$ and $M(8)$ octahedra showed considerable

TABLE 5a. INTERATOMIC DISTANCES IN ORTHOPINAKIOLITE (Å)**

M(1)***		M(5)		M(7*)		M(9)	
square plane		-O(1)	2.008(4)	-O(7)	2.019(9) × 2	-O(10)	2.054(4) × 2
-O(1)	1.983(4) × 4	-O(6)	2.085(4)	-O(8)v	2.10(1)	-O(12)	2.113(6)
elongate vertices		-O(2)	2.094(4)	-O(3)	2.39(2)	-O(6)	2.117(6)
-O(16)iv	2.177(5) × 2	-O(3)	2.113(4)	-O(4)	2.40(1) × 2	-O(7)	2.169(4) × 2
average	2.048	-O(5)	2.133(4)	-O(12)	2.89(2)	average	2.113
		-O(7)	2.149(4)	average	2.317		
M(2)***		average	2.075			M(10)	
square plane				M(7̄)		-O(10)	1.985(4)
-O(1)	1.980(4) × 4	M(6)***		-O(4)	1.916(5)# × 2	-O(8)	2.088(4)
elongate vertices		square plane		-O(3)	2.020(9)#	-O(13)	2.090(4)
-O(15)iv	2.180(6) × 2	-O(4)	1.908(4) × 2	-O(13)iv	2.30(3)#	-O(14)	2.099(4)
average	2.047	-O(7)	1.917(4) × 2	-O(8)v	2.84(2)	-O(4)vi	2.123(4)
		elongate vertices		-O(7)	2.93(2) × 2	-O(9)	2.130(4)
M(3)***		-O(9)v	2.261(6)	average	2.408	average	2.086
square plane		-O(2)	2.330(6)	#average of four			
-O(4)	1.913(4) × 4	average	2.040	1.998		M(11)	
elongate vertices						-O(10)	2.041(4)
-O(14)iv	2.252(5) × 2	M(7)		M(8)***		-O(1)vi	2.045(4)
average	2.026	-O(4)	2.043(4) × 2	square plane		-O(16)	2.072(4)
		-O(3)	2.126(7)	-O(10)	1.905(4) × 2	-O(11)	2.091(4)
M(4)		-O(8)v	2.340(7)	-O(7)	1.963(4) × 2	-O(15)	2.091(4)
-O(4)	2.225(4) × 4	-O(7)	2.396(5) × 2	elongate vertices		-O(12)	2.114(4)
-O(13)iv	2.205(6)	average	2.224	-O(5)	2.192(6)	average	2.073
average	2.218			-O(11)	2.349		
				average	2.046		

B(1)		B(2)		B(3)		B(4)	
-O(2)	1.364(9)	-O(15)iv	1.37(1)	-O(12)	1.37(1)	-O(6)	1.370(10)
-O(16)iv	1.385(9)	-O(13)iv	1.38(1)	-O(5)	1.39(1)	-O(9)	1.382(9)
-O(14)iv	1.391(9)	-O(3)	1.40(1)	-O(8)	1.40(1)	-O(11)v	1.393(10)
average	1.380	average	1.38	average	1.38	average	1.382

** Estimated standard errors in parentheses refer to the last digit. i = -x, -y, -z;
   ii = -x, -y, z; iii = x, y, -z; iv = 1/2+x, 1/2-y, 1/2-z; v = 1/2-x, 1/2+y, 1/2+z;
   vi = 1/2-x, 1/2+y, 1/2-z.

*** Mn^{3+}

(a)

(b)
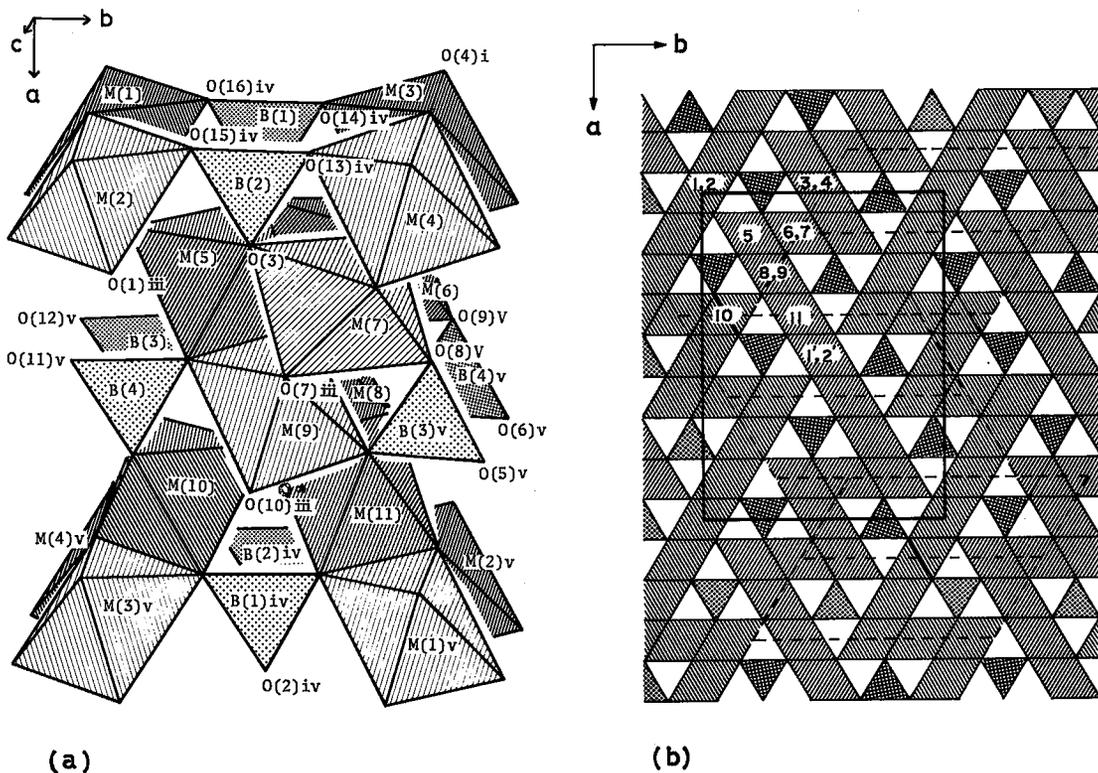
FIG. 2. (a) The structure of orthopinakiolite in a quarter cell, $a/2$, $b/2$ and c (a view down the axis lying at an angle of 108.4° to a and 96.4° to b). (b) Idealized arrangement of octahedral columns (ruled) and BO_3 triangles (stippled) projected down the c axis. Broken lines trace the monoclinic cell of pinakiolite (Fig. 7a), of which orthopinakiolite represents a twinned form.

O⁻ were taken from vol. IV of the *International Tables for X-ray Crystallography*. We give final positional parameters in Table 3, and aniso-tropic thermal parameters in Table 4; the occu-pancies at each cation position are listed in Table 2. The high temperature-factors of $M(4)$, $M(7*)$ and $M(\tilde{7})$ are probably due to the partial occupations of these sites. As the octahedron about $M(4)$ is relatively large (Table 5a), we assumed a distribution of Mn^{2+} and Mg in this position and refined their occupancy parame-ters. The result, however, showed that Mg was dominant (Table 2); the high temperature-factor of $M(4)$ may be due in part to positional dis-order of Mg in the large octahedron for this atom.

DISCUSSION OF THE STRUCTURE

The arrangement of octahedral columns

Like those of pinakiolite and related borates, the structure of orthopinakiolite consists of in-finite columns of edge-sharing octahedra where the shared edges are normal to the column direction, parallel to the fibre axis (c). These columns are laterally joined by sharing edges to form the structure (Fig. 2). The structure may be regarded as composed of: (i) 'flat' walls, like the one made of columns $M(5)$, $M(8,9)$, $M(11)$ and their inversion images plus $M(1',2')$; (ii) 'corrugated' walls, each consisting of $M(3,4)$, $M(6,7)$ and the inversion image of the latter, and (iii) columns like $M(10)$, which are flanked on wall (ii) to form Z-shaped walls. The two types of walls, (i) and (ii), will be designated as F and C walls respectively.

Whereas F walls in orthopinakiolite are seven octahedra wide, in pinakiolite they form a con-tinuous sheet parallel to (100). Likewise, C walls in pinakiolite form with columns of (iii) continuous equilateral zig-zag sheets parallel to (100). These two kinds of sheets alternate in pinakiolite. In contrast to this, a F wall and a Z-shaped wall in orthopinakiolite join, by sharing edges, to form a continuous irregular

TABLE 5b. INTERATOMIC DISTANCES (Å) AND O(i)-M-O(j) ANGLES (°) IN ORTHOPINAKIOLITE

```
M(1)***                            O(3)-O(7)          2.949(6)  87.6   average            2.892     89.9
square edges                       O(2)-O(3)          3.034(1)  92.3
O(1)-O(1)ii   × 2  2.550(7)  80.0  O(5)-O(6)          3.039(1)  92.2   M(9)
O(1)-O(1)iii  × 2  3.039(9) 100.0  O(1)-O(5)          3.040(6)  94.4   O(7)-O(10)  × 2  2.666(5)  78.2
elongate edges                     O(1)-O(2)          3.066(6)  96.7   O(6)-O(7)   × 2  2.818(6)  82.2
O(1)-O(16)iv  × 4  3.128(6)  97.4  O(1)-O(6)          3.077(6)  97.5   O(10)-O(12) × 2  2.818(6)  85.1
O(1)-O(16)v        2.750(6)  82.6  O(1)-O(3)          3.090(6)  97.1   O(7)-O(12)  × 2  3.128(6)  93.9
average            2.891     90.0  average            2.955     89.8   O(6)-O(10)  × 2  3.169(6)  98.9
                                                                       O(10)-O(10)iii   3.181(9) 101.5
M(2)***                            M(6)***                             O(7)-O(7)iii     3.372(8) 102.1
square edges                       square edges                       average          2.979     90.0
O(1)-O(1)ii   × 2  2.550(7)  80.2  O(4)-O(4)iii       2.607(5)  86.2
O(1)-O(1)iii  × 2  3.029(9)  99.8  O(7)-O(7)iii       2.696(9)  89.4   M(10)
elongate edges                     O(4)-O(7)    × 2   2.755(5)  92.2   O(4)vi-O(9)      2.741(6)  80.3
O(1)-O(15)iv  × 4  3.110(6)  96.7  elongate edges                     O(4)vi-O(14)     2.754(6)  81.4
O(1)-O(15)v   × 4  2.769(6)  83.3  O(4)-O(9)v   × 2   2.741(6)  81.8   O(8)-O(13)       2.858(8)  86.3
average            2.890     90.0  O(2)-O(7)    × 2   2.800(6)  81.9   O(4)vi-O(8)      2.869(6)  85.9
                                   O(2)-O(4)    × 2   3.156(6)  95.7   O(9)-O(14)       2.895(8)  86.4
M(3)***                            O(7)-O(9)v   × 2   3.221(7) 100.6   O(4)vi-O(13)     2.955(6)  89.1
square edges                       average            2.887     90.0   O(10)-O(13)      3.005(7)  95.0
O(4)-O(4)ii   × 2  2.799(7)  94.1                                      O(13)-O(14)      3.034(1)  92.8
O(4)-O(4)iii  × 2  2.607(8)  85.9  M(7)                                O(8)-O(9)        3.037(1)  92.1
elongate edges                     O(4)-O(7)    × 2   2.755(5)  76.3   O(10)-O(14)      3.039(6)  96.2
O(4)-O(14)iv  × 4  3.142(6)  97.6  O(4)-O(8)v   × 2   2.869(6)  81.5   O(8)-O(10)       3.041(7)  96.6
O(4)-O(14)v   × 4  2.754(6)  82.4  O(3)-O(7)    × 2   2.949(6)  81.2   O(9)-O(10)       3.052(7)  95.7
average            2.866     90.0  O(7)-O(8)v   × 2   3.304(7)  88.5   average          2.940     89.8
                                   O(3)-O(4)    × 2   3.325(7) 105.8
M(4)                               O(7)-O(7)iii       3.372(8)  89.4   M(11)
square edges                       O(4)-O(4)iii       3.461(8) 115.8   O(1)vi-O(16)     2.750(6)  83.8
O(4)-O(4)ii   × 2  2.799(7)  77.9  average            3.103     89.3   O(1)vi-O(15)     2.769(6)  84.0
O(4)-O(4)iii  × 2  3.461(8) 102.1                                      O(10)-O(12)      2.818(6)  85.4
elongate edges                     M(8)***                             O(10)-O(11)      2.846(6)  87.5
O(4)-O(13)iv  × 4  3.301(6)  96.3  square edges                       O(12)-O(16)      2.867(8)  86.5
O(4)-O(13)v   × 4  2.955(6)  83.7  O(7)-O(10)   × 2   2.666(5)  87.1   O(11)-O(15)      2.868(8)  87.0
average            3.129     90.0  O(7)-O(7)iii       2.696(9)  86.8   O(10)-O(15)      2.964(6)  91.7
                                   O(10)-O(10)iii     2.887(9)  98.5   O(1)vi-O(11)     3.019(6)  94.2
M(5)                               elongate edges                     O(10)-O(16)      3.020(6)  94.5
O(5)-O(7)          2.779(7)  80.9  O(5)-O(7)    × 2   2.779(7)  83.8   O(15)-O(16)      3.034(1)  93.6
O(2)-O(7)          2.800(6)  82.6  O(10)-O(11)  × 2   2.846(6)  83.3   O(11)-O(12)      3.039(1)  93.1
O(6)-O(7)          2.818(6)  83.4  O(7)-O(11)   × 2   3.114(6)  92.0   O(1)vi-O(12)     3.161(6)  98.9
O(3)-O(6)          2.821(8)  84.4  O(5)-O(10)   × 2   3.153(7) 100.4   average          2.930     90.0
O(2)-O(5)          2.943(8)  88.2

B(1)                               O(3)-O(13)iv       2.396(8) 119.7   average          2.397    120.0
O(2)-O(16)iv       2.384(8) 120.2  O(13)-O(15)        2.398(8) 121.8
O(14)-O(16)        2.386(8) 118.5  average            2.390    120.0   B(4)
O(2)-O(14)iv       2.402(8) 121.3                                      O(6)-O(9)        2.387(8) 120.4
average            2.391    120.0  B(3)                                O(9)-O(11)v      2.394(8) 119.3
                                   O(5)-O(12)v        2.373(8) 118.8   O(6)-O(11)v      2.397(8) 120.4
B(2)                               O(5)-O(8)          2.399(8) 119.1   average          2.393    120.0
O(3)-O(15)iv       2.377(8) 118.5  O(8)-O(12)v        2.420(8) 122.0
```

The maximum estimated error in O-M-O angles is ±0.02° excepting the cases M = B in which the maximum error is ±0.07°. The angles about M(7*) and M(7̃) are not given. The symmetry code is explained in TABLE 5a. Triple asterisks denote Mn3+.

FIG. 3. Comparison of cation arrangements in the F walls of orthopina-
kiolite (a) and pinakiolite (b), each being projected along a normal to
the wall. Note the distortion of $M(9)$ octahedra in the former. Shaded
small circles represent Mn^{3+}.

zig-zag sheet parallel to (100). They are linked, by sharing corners, with similar neighbors to build up the octahedral framework. In the interstices of such a patchwork of irregular zig-zag sheets, [BO$_3$]$^{3-}$ triangles lie perpendicular to the c axis.

Octahedral columns in the F wall share edges which are oblique to the fibre axis, whereas in the C wall the shared edges between adjacent columns are parallel to the fibre axis. It follows that the scheme of cation order and the mode of distortions are different in these two types of walls, as will be discussed in subsequent paragraphs. This effect is of fundamental importance to characterize both orthopinakiolite and pinakiolite structures. Moore & Araki (1974) discussed it in considerable detail for the pinakiolite structure.

From the characteristic shape of the elongate square bipyramid, we conclude that $M(1)$, $M(2)$, $M(3)$, $M(6)$ and $M(8)$ are occupied by Mn^{3+} (Table 2). The bond lengths and edge lengths of the polyhedra are listed in Table 5.

Ordering scheme in the F wall

The arrangement of atoms in the F wall of orthopinakiolite (Fig. 3a) and of pinakiolite (Fig. 3b) shows that both walls share the same feature where octahedral columns of Mn^{3+} and of divalent atoms alternate. However, in the orthopinakiolite F wall, there is a pair of columns in which Mn^{3+} and Me^{2+} alternate along the fibre axis. The $M(9)$ position, which accommodates the divalent cation, contains 0.57 Mg and 0.43 Mn^{2+}. The facts that the $M(9)$ octahedron shows no elongation and that the average bond length (Table 5) has a value expected for the refined contents confirm the

proposed distribution. The octahedron is distorted owing to geometrical restriction (Fig. 4) in such a way that it will not admit Mn^{3+}, which surrounds itself with a tetragonally distorted octahedron.

As pointed out by Moore & Araki (1974), the shortest shared edges occur between Mn^{3+} square bipyramids. Accordingly, square planes of the Mn^{3+} polyhedra in the F wall tend to elongate along the fibre axis. However, as no edge sharing between the square planes and the Me^{2+} octahedra occurs in the F wall, the Jahn-Teller distortion about Mn^{3+} admits less severe geometrical restriction to neighboring Me^{2+} octahedra in the F wall than in the C wall.

(a)

(b)
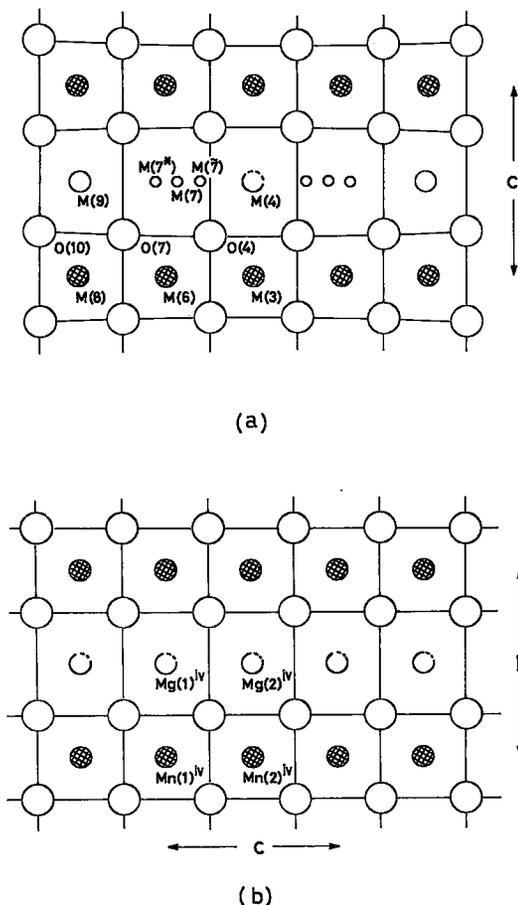
FIG. 4. Comparison of cation arrangements in the C walls of orthopinakiolite (a) and pinakiolite (b), each being projected along a normal to the wall. Shaded medium circles represent Mn^{3+} and small circles 'split atoms'; partly broken circles indicate the partly vacant sites. The pair of rim columns in (a) belong to F walls.

Ordering scheme in the C wall

The cation distribution in the C wall of orthopinakiolite (Fig. 4a) and of pinakiolite (Fig. 4b) shows that, in contrast to the F-wall case, Mn^{3+} atoms occur in alternate octahedral sites along each column, and at the same z level. Each Mn^{3+} square bipyramid thus shares a pair of square edges with those of bipyramids in adjacent columns, forming a lateral array of edge-sharing Mn^{3+} bipyramids. The other pair of square edges is shared by adjacent octahedra in the same column. Consequently, the square is considerably contracted, particularly parallel to c, giving very short Mn^{3+}–O (square) bonds. The shortest bond length, 1.913(4) Å, which occurs in $M(3)$, is shorter by three percent than the average Mn^{3+}–O (square) bond length in the F wall.

The contraction of the square is compensated by substantial expansion of octahedra adjacent to Mn^{3+} in the same column (Table 5). In agreement with the pinakiolite case (Moore & Araki 1974), vacancies in our structure occur only in the C wall, but particularly at $M(4)$, which is about 40% empty (Fig. 4). The $M(7)$ octahedron, however, which is adjacent to Mn^{3+} at $M(6)$ in the same column, does not possess any vacancy, but the octahedral atoms are split into three positions, $M(7)$, $M(7^*)$ and $M(\tilde{7})$ (Fig. 5); the $M(7) - M(7^*)$ and $M(7) - M(\tilde{7})$ distances are 0.70(2) and 0.77(1)Å respectively.
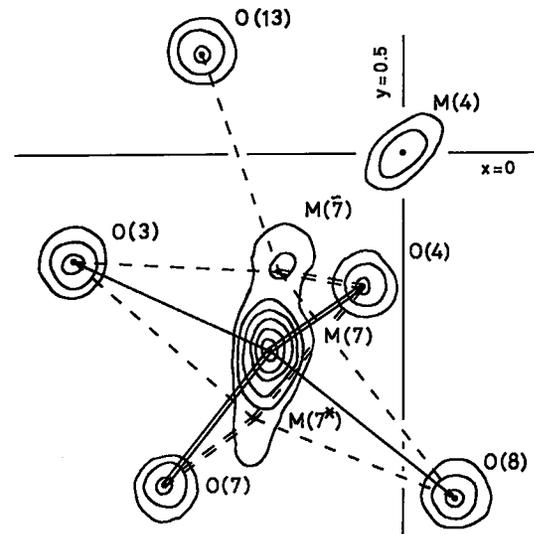
FIG. 5. Fourier peaks showing 'split atoms' $M(7)$, $M(7^*)$ and $M(\tilde{7})$ viewed along c. Contours are drawn with equal intervals of 10 eÅ^{-3} starting from 10 e contour.

This situation is likely the result of probable attainment of local charge balance around the large octahedral space. These octahedra are larger, compared to the corresponding ones in pinakiolite, primarily because the orthopinakiolite structure as a whole contains more Mn^{2+}.

The octahedral columns like $M(10)$ that flank the C wall to form the shape of a Z wall are mainly occupied by Mg, in both orthopinakiolite and pinakiolite, although Mg in these columns tends to be partly replaced by atoms of higher valence state other than Mn^{3+}. The octahedral columns into which Moore & Araki (1974) introduced Mn^{4+} in fact are columns of this kind.

The above scheme of cation distribution is primarily explainable from the electrostatic valence balance of anions in a way similar to that of pinakiolite (Moore & Araki 1974). In particular, regarding the distribution of Fe^{3+} in orthopinakiolite, we assigned 0.294(9) Fe^{3+} at $M(\tilde{7})$ because of the tetrahedral coordination about $M(\tilde{7})$ (Fig. 5) and evenly distributed the remaining Fe^{3+} atoms over the $M(10)$ and $M(11)$ sites. With these assignments, the anions in the orthopinakiolite structure as a whole show a satisfactory valence balance.

RELATIONSHIPS BETWEEN ORTHOPINAKIOLITE AND PINAKIOLITE

Structural relationship

The basic geometrical features of the pinakiolite substructure (Takéuchi *et al.* 1950), as characterized by links of octahedra and triangles, are the same as those of the ordered true structure (Moore & Araki 1974). Accordingly, the structural relationship between orthopinakiolite and pinakiolite may well be studied based on the substructure, which is the structure type of hulsite (Moore & Araki 1974, Konnert *et al.* 1976). The non-reduced monoclinic cell which Takéuchi *et al.* (1950) used to describe the substructure indeed has a periodicity of 12.73Å, similar to $b = 12.45$Å of the ludwigite cell (Takéuchi *et al.* 1950). As the fibre axes of all are also of similar periodicity (3Å, except for doubling due to cation order), essential differences in their cell dimensions are observed only in one direction.

A closer examination of these structures has revealed that the orthopinakiolite structure can be described as an Ito twin (Ito *et al.* 1950) of the pinakiolite substructure on the scale of a cell with a doubled (Fig. 2); such a relation was predicted by Strunz (1970) based on cell dimensions. The Ito twin operation is a glide reflec-
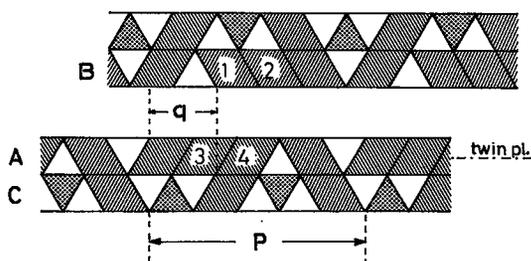
FIG. 6. Three types of layers A, B and C; the first two consist of octahedral columns and the third consists of octahedral columns and BO_3 triangles. The upper layers are related to the lower ones by a glide reflection, the reflection plane being parallel to the layer and having glide component $q = 3P/10$. In deriving the orthopinakiolite structure (Fig. 2b) by polysymmetric synthesis, layers such as A and B at a twin position overlap across a twin plane, as indicated. In this case pairs of columns such as 1, 2 and 3, 4 do not coincide; to form the structure, the pair 1, 2 must change its orientation to that of the other pair 3, 4.
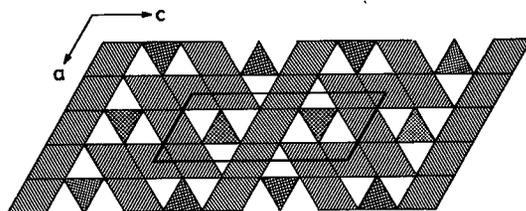
(a)
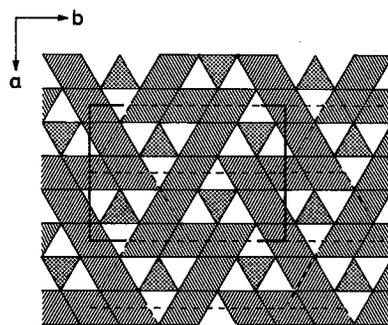
(b)

FIG. 7. (a) Idealized structure of pinakiolite, showing the cell given by Takéuchi *et al.* (1950). (b) Idealized structure of ludwigite depicted as a polysynthetic twin of the idealized pinakiolite structure that takes place on the unit-cell scale. Broken lines trace the monoclinic cell of pinakiolite, the horizontal lines corresponding to the twin planes.

tion in a plane parallel to (100), with a glide component of $\pm 3P/10$ ($-3P/10 \equiv 7P/10$). Here, P corresponds to c of the pinakiolite subcell, and is equal to five times the edge of the rhombus or triangle as illustrated in Figures 2b and 6; the glide component equals 1.5 times the edge length.

The strips of rhombuses (or layers of octahedral columns parallel to (100)), like A and B in Figure 6, are astride the Ito twin plane that passes through the cations of the columns. In this case, specific pairs of rhombuses in a strip do not coincide with those in the other: those in one strip must change their orientation to coincide with corresponding ones of the other (Fig. 6). The structure thus has $a = 18.389$ Å, which agrees well with measured $a = 18.357$ Å.

A question arises: what will happen if the Ito twinning is considered not on the scale of double cell but on a unit-cell scale? The answer: the resulting structure is isotypic with ludwigite (Fig. 7).

Note that the structures of orthopinakiolite, pinakiolite and ludwigite consist of the three and only three kinds of layers (Fig. 6); the two rhombus layers A and B are enantiomorphs. Thus there is another way of looking at these structures: they are composed of stackings of these three kinds of layers, in which a rhombus layer of either kind alternates with a layer containing $[BO_3]^{3-}$. Depending upon the mode of stacking, various structures result. The Ito twin description, however, is the simplest one.

Mode of structural variation due to polysymmetric synthesis

It takes fewer columns of octahedra to constitute a C wall in orthopinakiolite than in pinakiolite (Table 6). The polysymmetric synthesis (Fig. 2) that leads to orthopinakiolite plays a role in reducing the number of columns in the C wall relative to that in the F wall. The amount of reduction depends on the size of the twin unit. If twinning takes place on the scale of a triple cell (a tripled), it yields a structure ($a = 27.54$ Å) in which F and C walls consist of nine and five columns respectively.

TABLE 6. DISTRIBUTION IN ORTHOPINAKIOLITE AND PINAKIOLITE OF Mn³⁺ AND HOLES IN THE F AND C WALLS*

	Mn³⁺		Hole		Octahedral columns involved (%)	
Walls	F	C	F	C	F	C
Orthopinakiolite	4	3	0	0.41	58	25
Pinakiolite	4	4	0	0.84	33	33

* Number per 40 oxygen atoms.

Accordingly in such a hypothetical structure, the C wall can accommodate more Mn^{3+} than in orthopinakiolite, though less than that in pinakiolite.

In general, when twinning takes place on the scale of n cells, the Mn^{3+} contents in the F and C walls of the resulting structure are respectively 4 and $2(2n-1)/n$ per twelve columns (Takéuchi 1978). Thus in the hypothetical orthopinakiolite-pinakiolite series, a change in structure from one phase to another, accompanying a change in chemical composition, seems to go along with twinning on the unit-cell level; the higher the twin periodicity, the greater is the Mn^{3+} content. That such twinning, with concomitant changes in composition, yields a chemical series of structures was first observed in the PbS–Bi₂S₃ system by Takéuchi & Takagi (1974). This 'tropochemical twinning' (Takéuchi 1978) may be regarded as a special case of 'chemical twinning' (in the sense of Andersson & Hyde 1974) that occurs in a given chemical system. Compared to Ito twinning which originally describes polymorphic relations (Ito *et al*. 1950), tropochemical twinning appears to have genetic significance (Takéuchi & Takagi 1974, Takéuchi 1978) although conclusive proof is reserved for future study.

In conclusion, orthopinakiolite should be regarded, not as a polymorph, but as a Mn^{3+}-deficient modification of pinakiolite. According to Randmets (1960), both minerals belong to about the same period of mineral formation at the Långban deposit although they are not intimately associated.

REFERENCES

ANDERSSON, S. & HYDE, B. G. (1974): Twinning on the unit cell level as a structure-building operation in the solid state. *J. Solid State Chem.* 9, 92-101.

BÄCKSTRÖM, H. (1895): Ett pinakiolit närstående mineral från Långban. *Geol. Fören. Förh.* **17**, 257-259.

BERTAUT, E. F. (1950): Structures des boroferrites. *Acta Cryst.* **3**, 473-474.

COPPENS, P. & HAMILTON, W. C. (1970): Anisotropic extinction corrections in the Zachariasen approximation. *Acta Cryst.* A26, 71-83.

FEDERICO, M. (1957): Breislakite. *Period. Mineral.* **26**, 191-214.

FLINK, G. (1890): Ueber Pinakiolith und Trimerit, zwei neue Mineralien aus den Mangangruben Schwedens. *Z. Krist.* **18**, 361-376.

IBERS, J. A. & HAMILTON, W. C., eds. (1974): *International Tables for X-ray Crystallography.* IV. *Revised and Supplementary Tables.* Int. Union Cryst., The Kynoch Press, Birmingham.

ITO, T., SADANAGA, R. & TAKÉUCHI, Y. (1950): *X-ray Studies on Polymorphism.* Maruzen, Tokyo.

KONNERT, J. A., APPLEMAN, D. E., CLARK, J. R., FINGER, L. W., KATO, T. & MIÚRA, Y. (1976): Crystal structure and cation distribution of hulsite, a tin-iron borate. *Amer. Mineral.* **61**, 116-122.

MOORE, P. B. & ARAKI, T. (1974): Pinakiolite, $Mg_2Mn^{3+}O_2[BO_3]$; warwickite, $Mg(Mg_{0.5}Ti_{0.5})$ $O[BO_3]$; wightmanite, $Mg_5(O) (OH)_5[BO_3]) \cdot nH_2O$: crystal chemistry of complex 3 Å wallpaper structures. *Amer. Mineral.* **59**, 985-1004.

RANDMETS, R. (1960): Orthopinakiolite, a new modification of $Mg_3Mn^{2+}Mn^{3+}_2B_2O_{10}$ from Långban, Sweden. *Ark. Mineral. Geol.* **2**, 551-555.

STRUNZ, H. (1970): *Mineralogische Tabellen,* 5th ed. Akad. Verlagsgesellschaft Geest & Portig K.-G., Leipzig.

TAKÉUCHI, Y. (1956): The crystal structure of vonsenite. Mineral. J. (Japan) **2**, 19-26.

———— (1972): The investigation of superstructures by means of partial Patterson functions. *Z. Krist.* **135**, 120-136.

———— (1978): 'Tropochemical twinning': a mechanism of building complex structures. *Rec. Prog. Nat. Sci. Japan* **3**, 153-181.

———— & TAKAGI, J. (1974): The role of twinning on composition in the $PbS-Bi_2S_3$ series. *Proc. Jpn. Acad.* **50**, 843-847.

————, WATANABÉ, T. & ITO, T. (1950): The crystal structures of warwickite, ludwigite and pinakiolite. *Acta Cryst.* **3**, 98-107.

VENKATAKRISHNAN, V. & BUERGER, M. J. (1972): The crystal structure of $FeCoOBO_3$. *Z. Krist.* **135**, 321-338.

YAMNOVA, N. A., SIMONOV, M. A. BELOV, N. V. (1975): Crystal structure of the Fe-Mg borate hulsite $(Fe^{2+}, Mg, Fe^{3+}, Sn)_3BO_3O_2$. *Sov. Phys. Cryst.* **20**, 89-90.